

# Evaluation of the Properties of Cement Mortars with the Addition of Thermoelectric Generation Waste

Daniele Ferreira Lopes\*, Sabrina Neves da Silva

Universidade Federal do Pampa (UNIPAMPA), Graduate Program in Materials Science and Engineering (PPCEM), Advanced Study Group in Energy Engineering (GREEN), Avenida Maria Anunciação Gomes de Godoy, 1650, CEP 96413-172, RS, Bagé, Brazil.

Corresponding author. Email address: [danielelopes.aluno@unipampa.edu.br](mailto:danielelopes.aluno@unipampa.edu.br)

---

**Abstract:** The partial cement replacement by solid wastes of thermoelectric generation in mortar formulations can contribute to environmental preservation and the development of more durable construction materials. This study aimed to evaluate the influence of Portland cement partial replacement by coal fly ash and flue gas desulphurization by-product on the cementitious mortars properties. The experimental methodology consisted of the residues characterization by X-ray diffraction, Raman spectroscopy, scanning electron microscopy and particle size analysis. Cylindrical blocks of mortar with a 50 × 100 mm dimensions and a 1: 3: 0.48 trace (cement: sand: water/cement) were prepared according with NBR 7215 standard. Cement was replaced, by mass, in the proportions of 6%, 16% and 26%. Comprehensive strengths (NBR 7215) were measured at 7, 14 and 28 days of wet cure. In addition, water absorption by capillarity test was performed (NBR 9722). The results were compared with a reference sample, that is, without residues. It has been shown that, mineralogically, the ashes contain mulita, quartz (mainly) and hematite and have 42.19 µm average diameter. Particle morphology is predominantly spherical containing some porosities. The by-product is a material rich in calcium sulfate and quartz traces with 17.8 µm average diameter and consists of agglomerated particles with varied morphology. The results showed that the replacement of 6% Portland cement by ashes improves the performance of mortars in terms of axial comprehensive strength and capillarity water absorption. For the mortars containing the by-product, the improvement in mechanical properties was not evinced.

**Key words:** coal fly ash; gas desulfurization; recycling; thermoelectric generation; cement mortars

---

## 1. Introduction

Concrete and mortar are the most widely used materials in construction due to their versatility and ease of handling. Mortar can be conceptualized as a material obtained from the mixture, in appropriate proportions, of inert materials of low granulometry and a paste with agglomerating properties. Mortar differs from concrete in the size of the aggregate that makes it up [1].

Buildings can present structural problems over time. When analyzing the extensive structural reconstruction and/or maintenance caused by premature failure during use, this information has been confirmed to be exacerbated by exposure to

corrosive environments. The decrease in the durability of a structure creates an environmental problem due to the waste of raw materials, the increase in waste generated and the greater consumption of energy and natural resources [2, 3].

In this context, over time, cementitious materials have been improved by the introduction of additives, in the form of plasticizers, setting retarders, among others, as well as pozzolanic or cementing additions that make up the mixture by replacing cement or adding to it. Thus, studying solutions that extend the useful life of structures and minimize the environmental impact generated by their production chain is a challenge for researchers and the target of research related to the construction sector [4, 5].

The addition of waste to cement mortar formulations has already been shown in the literature. The main advantages are gains in strength, even when the amount of cement in the mix is reduced. In terms of microstructure, they contribute to the development of a more defined matrix and a less porous structure, which makes it more resistant to attack by aggressive agents, improving its durability combined with greater mechanical strength. Additions include construction and demolition waste generated by the building industry [6], coconut fiber [7], rice husk ash [8], sugar cane bagasse ash [9] and coal fly ash [10-12].

As for the influence of curing time, the literature shows that at 28 days, mortars containing coal ash additions performed better in the axial compressive strength test. This means that there is no increase in reactions to help increase the performance of mortars with curing times longer than 28 days [13-15].

In Brazil, burning coal to generate energy in Thermal Power Plants (TPPs) generates around 3.24 million tons/year of solid waste, such as slag, coal ash (light and heavy) and the by-product of desulphurization of combustion gases, a process known as Flue Gas Desulphurization (FGD). Only a small fraction of the by-products generated in TPPs, around 30%, are reused, the rest being disposed of in an inappropriate manner. The development of technologies to reuse these by-products, in addition to minimizing disposal in unsuitable areas, increases the credibility of this type of generation in the eyes of the consumer market [16, 17].

The high volume of the waste in question and the potential pozzolanic activity of coal ash, proven by several researchers [16-19], indicate its suitability for use in cementitious matrices.

For ALTHEMAN et al [17], the addition of coal fly ash to cementitious matrices is essential in order to meet the requirements of the National Solid Waste Policy. The results found by the authors showed that the ash has pozzolanic activity and, when added to the cement matrices studied, increased mechanical strength. The authors developed mortars with 5%, 10% and 20% mass replacement of Portland cement with coal ash from aluminum production. PACHECO et al. [18] state that substitution levels of between 40 and 50% by mass of Portland cement with coal fly ash show slower chemical reactions of hydration, contributing little to the initial strengths, however, they indicate the material due to the reduction in clinker consumption. DUARTE et al. [19] carried out a study aimed at evaluating the behavior of concrete, in the hardened state, with partial substitution of Portland cement with coal ash from thermoelectric power plants at levels of 7%, 14% and 21%, in relation to the mass of cement, and a reference concrete. Tests were carried out on axial compression, water absorption by capillarity and by immersion at the age of 28 days. It was concluded that the axial compressive strength decreases as the amount of ash added to the mix increases. However, the values are above the minimum strength of 20 MPa recommended by the NBR6118 standard. The addition of ash did not affect water absorption by immersion or capillarity. SANTANA [20] evaluated the use of the FGD by-product as a mineral addition in concrete with a *fck* (feature compression know) of 25 MPa with 0%, 5%, 10% and 20% in relation to the mass of cement. It was shown that the mechanical strengths of the concrete mixes were either unaffected or increased as the content of the added residue increased.

Based on the literature presented here, the objectives of this study were to characterize fly ash and the FGD by-product from a TPP located in the city of Candiota-RS and to assess the influence of replacing Portland cement with this waste on the properties of cement mortars.

## 2. Materials and Methods

### 2.1 Materials

A cement classified as CP IV-32 according to NBR 5736 [21] was used in all the formulations. This CP was chosen because it is suitable for building structures buried in the ground. In addition, the Campanha region of Rio Grande do Sul, the site of this study, is home to thermal power plants and, as such, the regional atmosphere has high concentrations of sulphates.

The chemical and physical characterizations of the cement were provided by the manufacturer and are shown in Tables 1 and 2.

**Table 1.** Chemical composition of CP IV-32 Portland cement

Tests	Results	References
Loss of fire - PF	3.34%	NBR NM 18 (ABNT, 2004) [22]
Silicon dioxide - SiO <sub>2</sub>	28.94%	NBR NM 11-2 (ABNT, 2004) [23]
Aluminum oxide - Al <sub>2</sub> O <sub>3</sub>	9.97%	
Iron oxide - Fe <sub>2</sub> O <sub>3</sub>	3.72%	
Magnesium oxide - MgO	3.18%	
Calcium oxide - CaO	45.12%	
Insoluble residues - R.I.	25.25%	NBR NM 15 (ABNT, 2004) [24]
Free calcium oxide	0.74%	NBR NM 13 (ABNT, 2004) [25]

**Table 2.** Physical characterization of CP IV-32 Portland cement

Tests	Results	References
Specific mass	2.83 g/cm <sup>3</sup>	NBR NM 23 (ABNT, 2001) [26]
Specific area	4,340 cm <sup>2</sup> /g	NBR NM 76 (ABNT, 1998) [27]
Blaine fineness	4.290 cm <sup>2</sup> /g	NBR NM 11579 (ABNT, 1991) [28]
Normal consistency paste water	30.3%	NBR NM 43 (ABNT, 2003) [29]
Start of setting	3.4 h	NBR NM 65 (ABNT, 2003) [30]
End of setting	4.25 h	
Le chatelier expansion - hot	0.34 mm	NBR NM 11582 (ABNT, 1991) [31]
Compressive strength 1 day	-	NBR 7215 (ABNT, 2019) [32]
Compressive strength 3 days	> 10.0 MPa	
Compressive strength 7 days	> 20.0 MPa	
Compressive strength 28 days	> 32.0 MPa	

The fine aggregate used was fine sand with a maximum particle size of 1 mm (NBR 7211 [33]). The mixing water came from the local sewage system in the city of Bagé-RS. The CP was partially replaced by fly ash (CV) and the FGD by-product (SP) provided by the Candiota Thermoelectric Complex. The waste was not prepared or handled in any way prior to being added to the mortar.

### 2.2 Characterization of the materials

The mineral composition of the waste was determined by X-ray diffractometry (XRD) and Raman spectroscopy. These techniques have a high resolution for identifying minerals even at low concentrations. Both techniques provide information on the compounds, but the former also identifies the crystalline structures. The combination of techniques is useful in cases where XRD does not provide satisfactory structural information, for example due to a high concentration of glassy material [34].

The diffractometer used was a Rigaku ULTIMA IV, JP. It operated with Cu K $\alpha$  radiation, generated at 40 kV and 20 mA. The scanning range was 3° to 80° and the integration time was 2 s per point. The Raman spectra were measured on a confocal Raman spectrometer with a laser of ( $\lambda = 532$  nm), and a beam diameter of 1  $\mu$ m in the range of 5 to 1900 cm<sup>-1</sup>. The experimental spectra were compared with the RRUFF database (<http://rruff.info/>) [35] and the mineral phases were identified using the X-pert High Score Plus software. The morphology of the particles was analyzed by scanning electron microscopy (SEM) using a Jeol JSM - 6610LV microscope. The particle size analysis, NBR 7181 [36], assessed the dispersion of sizes and the average diameter of the particles. The test was carried out on a CILAS model 1190 LD laser granulometer, measured in liquid solution.

### 2.3 Formulations and preparation of the specimens

The specimens were prepared with mortar made up of one part cement, three parts standardized sand, by mass, and with a water cement ratio of 0.48 (1:3:0.48), in accordance with NBR 7215 [32]. Test specimens were prepared with CP substituted by CV or SP at 0, 6%, 16% and 26% by mass. Table 3 shows the formulations of the traces analyzed in the research.

**Table 3.** Reference trait and with CV and SP

Draft	Agglomerate mass			Sand (g)	Water (mL)	Water/Cement ratio	Cement consumption (kg/m <sup>3</sup> )
	Cement (g)	CV (g)	SP (g)				
0%	624	-	-	1,872	300	0.48	3,120
6%	586.56	37.44	-	1,872	300	0.48	2,932.8
16%	524.16	99.84	-	1,872	300	0.48	2,620.8
26%	461.76	162.24	-	1,872	300	0.48	2,308.8
6%	586.56	-	37.44	1,872	300	0.48	2,932.8
16%	524.16	-	99.84	1,872	300	0.48	2,620.8
26%	461.76	-	162.24	1,872	300	0.48	2,308.8

Figure 1 shows the mortars in the molds before wet curing (1a) and the same demolded after 24 hours of curing (1b).

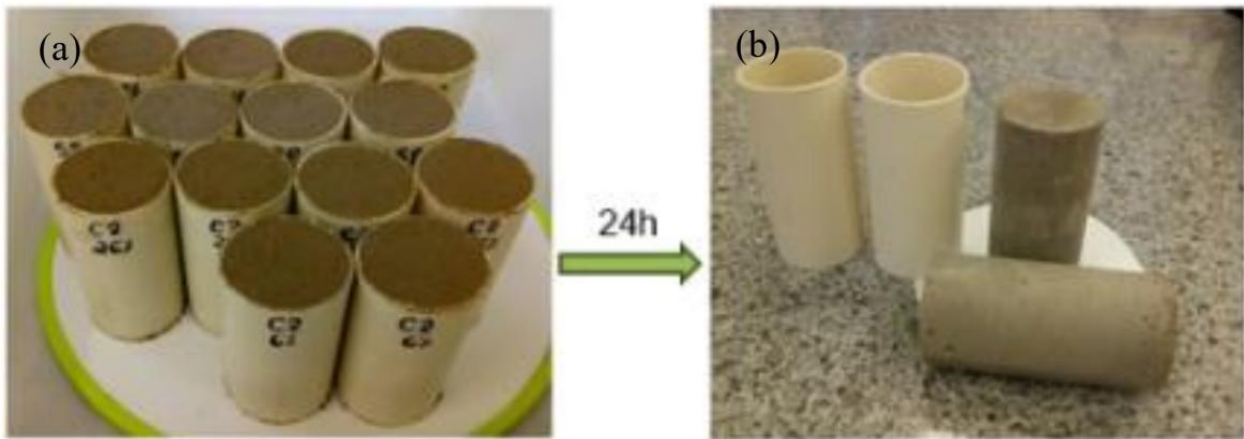


**Figure 1.** Specimens in (a) molds and (b) demolded after 24 hours.

#### 2.4 Compressive strength

The test method was carried out in accordance with NBR7215 [32], which involves determining the compressive strength of cylindrical specimens with a diameter of 50 mm and a height of 100 mm. EMIC model DL 20000 equipment was used with a load application speed of  $0.45 \pm 0.15$  MPa/s and a maximum load of 100 kN. The samples were compressed to failure at 7, 14 and 28 days of wet curing.

#### 2.5 Determination of water absorption by capillarity

This test is useful for monitoring the increase in mortar mass due to water absorption by capillarity in accordance with NBR 9779 [37]. Water absorption by capillarity was calculated using equation 1:

$$C = (A-B)/S \quad (1)$$

Where:  $C$  is the absorption of water by capillarity in  $\text{g}/\text{cm}^2$ ;  $A$  is the mass of the specimen that remains with one of its faces in contact with the water;  $B$  is the mass of the dry specimen and  $S$  is the cross-sectional area in  $\text{cm}^2$ .

#### 2.6 Statistical analysis

Analysis of variance (ANOVA) with a completely randomized design (DIC) was used to check for significant influences of the substitutions on the compressive strength response variable.

### 3. Results and Discussion

The diffractogram of VC, shown in Figure 3a, highlights an amorphous halo between  $15^\circ$  and  $35^\circ$ , which could indicate the pozzolanic activity of this residue, as indicated by HOPPE et al. [38] and YAN et al. [39].

In the mineralogical composition of the VC, phases of quartz ( $\text{SiO}_2$ ), mullite ( $\text{Al}_2\text{O}_3\text{-SiO}_2$ ) and traces of hematite ( $\text{Fe}_2\text{O}_3$ ) were identified, as shown in the diffractograms, Figure 3a, and the Raman spectrum, Figure 3b. According to the intensity of the peaks, quartz is most frequent, followed by mullite and hematite. This mineralogy was also found by KRÓL et al. [40] and AZEVEDO et al. [41]. Despite being from different locations, similarities were observed between the diffractograms, especially in the amorphous halo and the quartz peak between  $26^\circ$  and  $27^\circ$  [38-41]. The formation of mullite, identified only by XRD, is related to the combustion of coal at temperatures above  $1050^\circ\text{C}$ . Mullite is the phase that contributes to the material's mechanical strength [42].

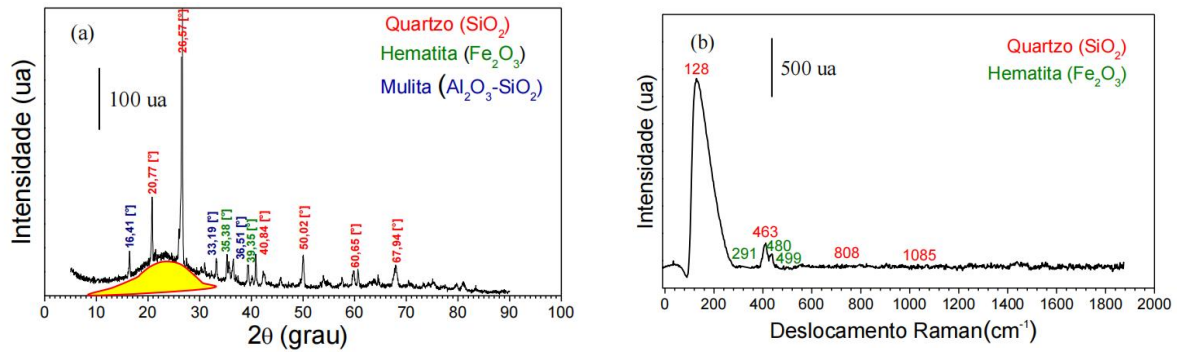


Figure 2. Diffractogram (a) and Raman spectrum (b) of VC.

When analyzing the SP diffractogram, a low degree of amorphism can be seen, due to the absence of an amorphous halo, and therefore the material has no pozzolanic activity. The material has a well-ordered structure, with well-defined peaks of intensity. In terms of mineral composition, the most significant phase is calcium sulphate (CaSO<sub>4</sub>·2H<sub>2</sub>O), in the form of gypsum and quartz, as shown in Figures 3a-b. Therefore, the residue cannot be considered pure. The quartz identified is due to the remaining VC that mixes with the SP during desulphurization. LI et al. [43] and FENG et al. [44] identified these compounds in FGD by-products.

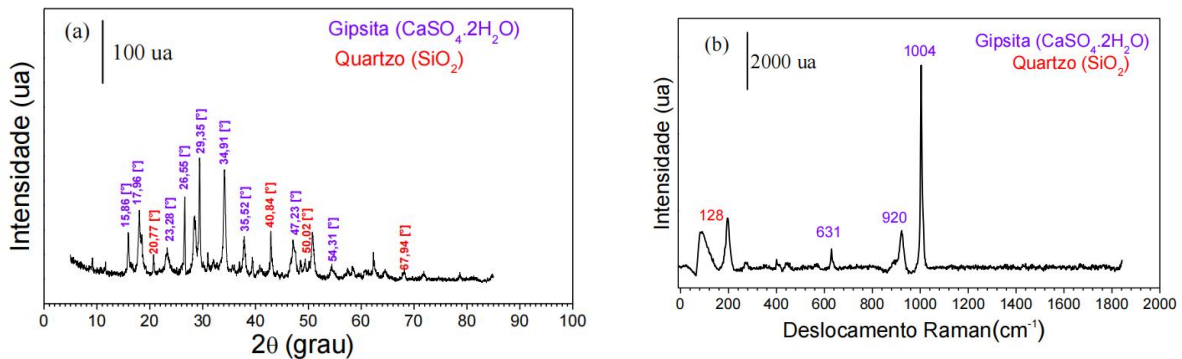


Figure 3. Diffractogram (a) and Raman spectrum (b) of SP.

In the SEM micrograph of the VC, Figure 4a, we can see particles with a diameter ranging from 0.7 μm to 20 μm, spherical morphology with a smooth surface (the majority) and some with microporosity. Spherical morphology is typically identified in fly ash from the combustion of pulverized coal, as reported in the literature [45, 46].

In the SP particles, Figure 4b, agglomerates with varied morphology are observed, containing some flaky crystals and prismatic-rhombic particles of varying size and heterogeneous distribution, consistent with the morphology observed by other authors [47, 48].

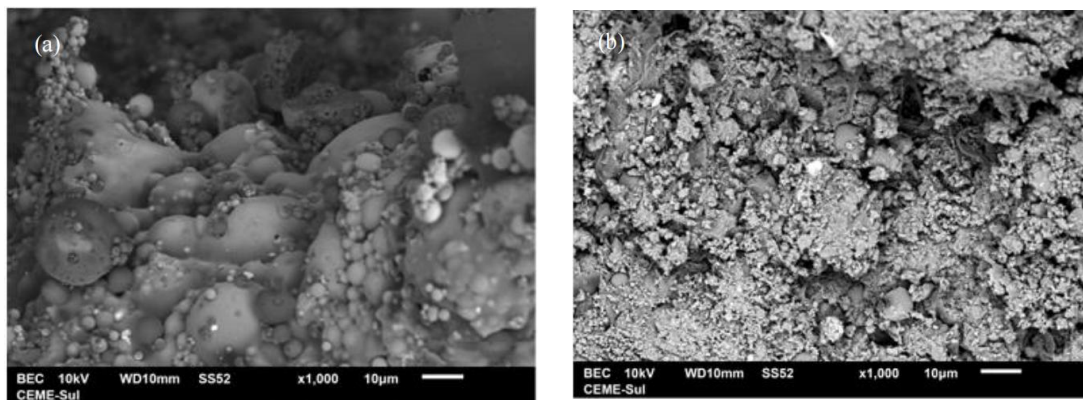
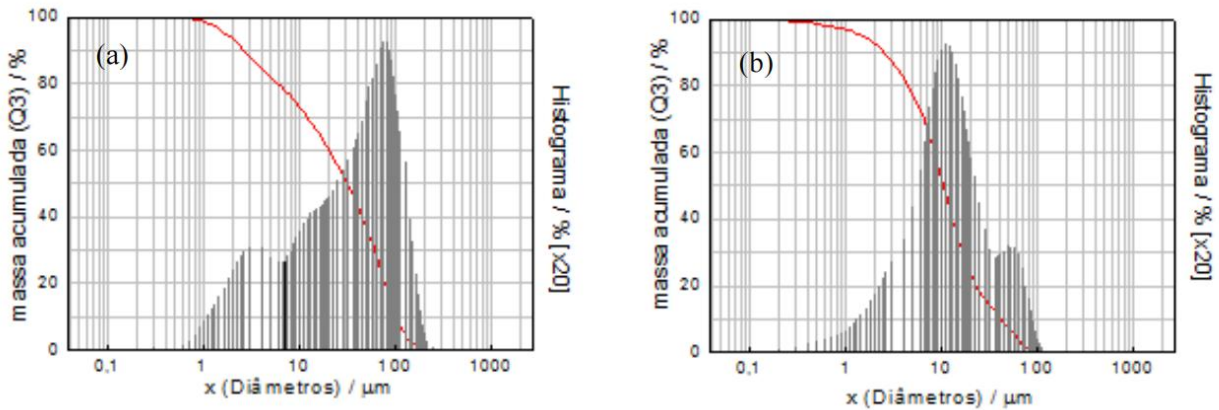


Figure 4. SEM images of (a) CV and (b) SP.



Figure 5 shows the particle size distribution of the waste. The x-axis of the diagrams shows the diameters in  $\mu\text{m}$ , the y-axis on the left shows the cumulative mass % and the y-axis on the right shows the histogram.

Average diameters of  $42.19 \mu\text{m}$  and  $17.83 \mu\text{m}$  were measured for CV and SP, respectively.

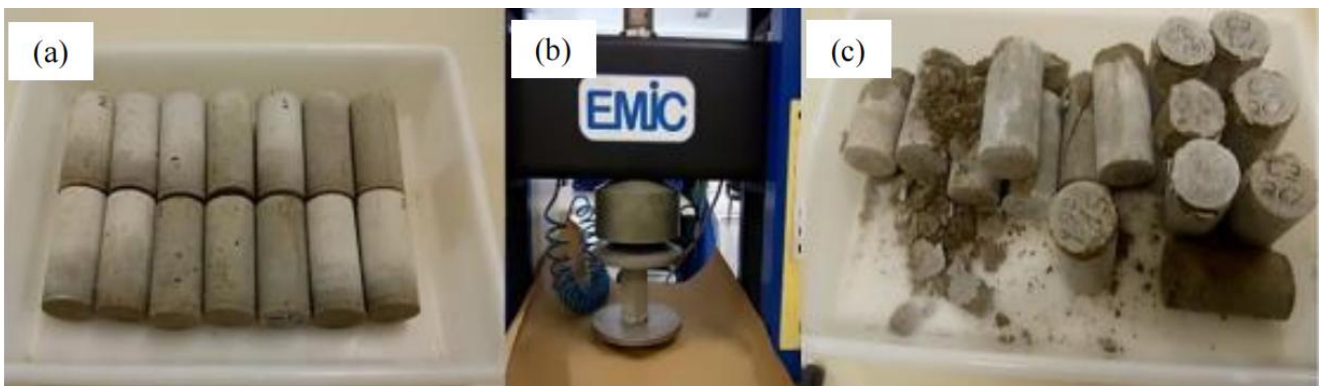


**Figure 5.** Particle size distribution (a) CV and (b) SP.

According to MEHTA and MONTEIRO [49], fly ash can have a diameter ranging from  $1 \mu\text{m}$  to  $100 \mu\text{m}$ . COSTA [50] obtained an average diameter of  $41.35 \mu\text{m}$ , while LACERDA [51],  $54.22 \mu\text{m}$ , both for fly ash from coal combustion at the same TPP that supplied the material for this study. The differences between the average diameter found in this work and those of other authors [50, 51] are related to the characteristics of the combustion process and the coal burned [52].

ZERBINO et al. [53] highlight the importance of the particle size distribution of the waste in terms of the performance of the paste that incorporates it. In the case of concrete containing ash, with a replacement content of 15% by mass, the authors observed improvements in the fresh state properties and also in the mechanical properties and durability. This is due to the greater fineness of the material. According to ZERBINO et al. [53], ash can even influence the inhibition or development of the alkali-silica reaction (ASR). The mitigation or exacerbation of the ASR depends on the replacement content of the cement and, above all, the particle size of the added material.

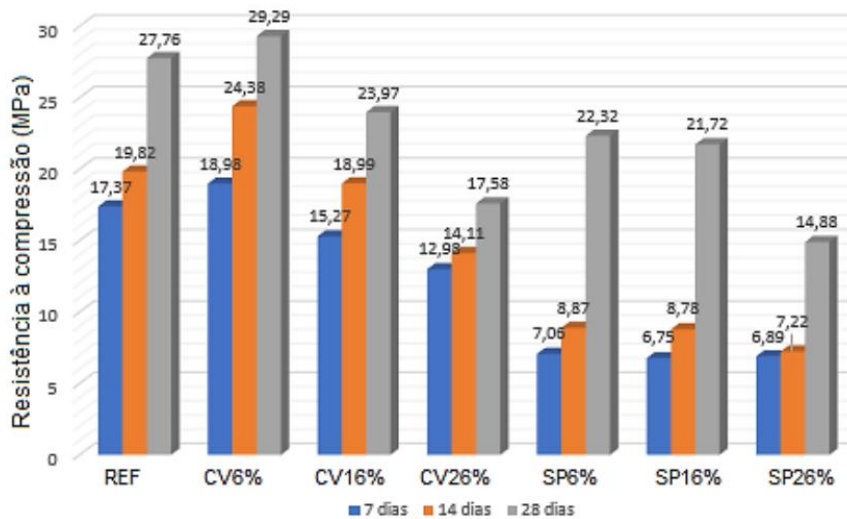
Figure 6 shows the specimens before the axial compressive strength test (6a), positioned in the equipment (6b) and broken (6c). Table 5 shows the axial compressive strength values of the mortar specimens molded with different levels of cement replacement with waste after 7, 14 and 28 days of curing. These values correspond to the average of three measurements. Graphically, the results are shown in Figure 7.



**Figure 6.** Mortars (a) before (b) during and (c) after compressive strength measurement.

**Table 5.** Axial compressive strength of cementitious mortars

Clay	Axial compression strength (MPa)		
	7 days	14 days	28 days
REF	17.37	19.81	27.76
6% CV	18.98	24.36	29.29
16% CV	15.27	18.99	23.97
26% CV	12.98	14.11	17.58
6% SP	7.06	8.87	22.32
16% SP	6.75	8.78	21.72
26% SP	6.89	7.22	14.88

**Figure 7.** Axial compressive strength of cementitious mortars.

Analysis of the results showed that the strengths were higher at 28 days of curing. With regard to the replacement content, the greatest gain was for the mortar with a 6% CV cement replacement content. According to HOANG et al [54], the initial strengths at younger ages are lower due to the lower clinker content and the late reactions of the pozzolanic material. In addition to its chemical effect, replacing cement with pozzolanic material also reduces the pore size of the cement matrix [55]. The strength gain for this formulation, i.e. with 6% CV, was 1.53 MPa. This value can be considered small, but the material is recommended due to the reduction in cement consumption of 187.2 kg/m<sup>3</sup>.

In relation to the specimens containing SP, there was no gain in strength at the replacement levels and curing times analyzed in this study. In the work carried out by KHATIB et al. [56], which evaluated the replacement of cement with FGD residue in concrete in mass percentages ranging from 10% to 90% at curing times of 1, 7, 28 and 365 days, the addition of residue contributed to a gain in compressive strength only for concrete containing 10% residue at 365 days of curing. In the other conditions, the results were lower than the reference concrete. In the flexural strength tests, the gain was limited to the 30% replacement content at 28 days of curing. Possibly due to the addition of this waste, expansive (deleterious) products are formed, which generate internal stresses in the material.



For statistical analysis, three factors were considered: type of mortar (A), curing time (B) and percentage cement replacement content (C). Factor A had two levels, factor B had three levels and factor C had four levels. The factorial design was carried out with two replicates. The distribution of the data for the analysis is shown in Table 6.

**Table 6.** Data for general factor analysis

Type of clay (a)	Curing time (B)											
	7 days				14 days				28 days			
	Percent cement replacement content (C)											
	0%	6%	16%	26%	0%	6%	16%	26%	0%	6%	16%	26%
Containing CV	16.89 17.85	18.25	14.99	14.83	19.22 20.42	24.60	20.42	13.69	27.45 28.07	30.26	23.20	17.21
		19.71	15.55	11.13		24.12	17.56	14.53		28.32	24.74	17.96
7.59		5.98	6.01	7.99		8.02	8.12	21.54		22.94	15.80	
6.53		7.52	7.77	9.74		9.54	6.32	23.10		20.50	13.96	
Containing SP												

The factorial design showed that the first-order factors (A, B and C) and the second-order factors (AC and BC) were significant. It was observed that time, factor B, interacted with the mortar mix used and with the replacement content used (factor C).

As it was clear that time was influencing the results, it was decided to carry out this analysis separately, using only factors B and C. Table 7 shows the ANOVA results for a) 7, b) 14 and c) 28 days of wet curing.

**Table 7.** ANOVA for a) 7 days b) 14 days and c) 28 days

a) ANOVA (7 Days)	Sum quadratic	Mean quadratic	F	P-value	F crit
Type of mortar	175.9602	175.9602	114.5798	5.096E-06	5.317655
% content	129.3643	43.12143	28.07933	0.0001343	4.066181
Interaction	75.80467	25.26823	16.45388	0.0008775	4.066181
Total	381.1292				
b) ANOVA (14 Days)	Sum quadratic	Mean quadratic	F	P-value	F crit
Type of mortar	265.6085	265.6085	206.2127	5.400E-07	5.317655
% content	182.5067	60.8355	47.2314	1.964E-05	4.066180
Interaction	126.2027	42.0675	32.6603	7.744E-05	4.066180
Total	574.3179				
c) ANOVA (28 Days)	Sum quadratic	Mean quadratic	F	P-value	F crit
Type of mortar	35.55141	35.55141	27.40085	0.0007885	5.317655

% content	304.982	101.6 607	78.35383	2.85E-06	4.066181
Interaction	25.40902	8.469673	6.527906	0.0152519	4.066181
Total	365.9424				

In the diagram relating the variation in compressive strength to the percentage additions (Figure 8), it can be seen that the addition of 6% CV is associated with the highest average strength, indicating that this main effect is significant in the response variable (gain in strength at 28 days). It can also be seen that with the higher substitutions, 16 and 26%, there was a decrease in strength. The diagrams shown in Figure 8 emphasize that for all the additions studied, VC gave the mortars greater strength compared to SP and also that the mortar containing 6% VC had the highest strength of all the situations evaluated.

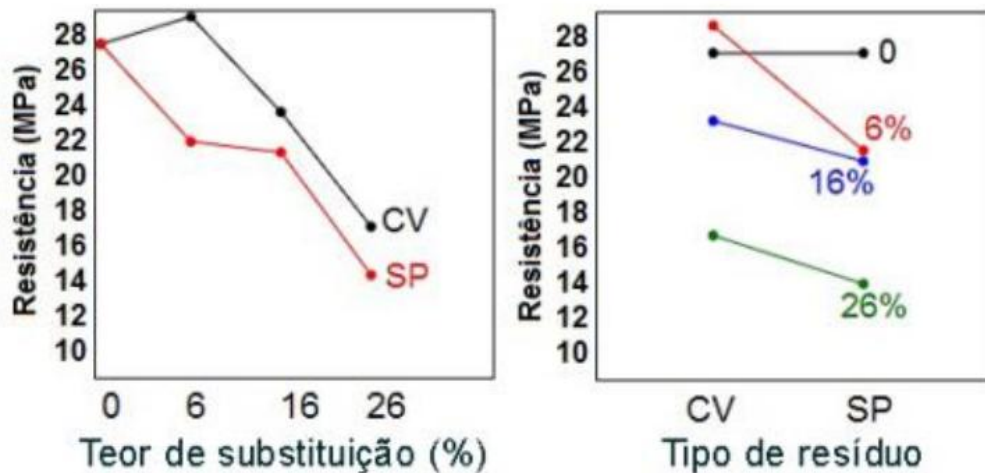


Figure 8. Effects of additions on mechanical strength.

Water absorption by capillarity decreased for the mortar with a 6% CV replacement content. This can be explained by the refinement of the pores due to the addition of the residue. However, this value still does not meet the requirements of NBR 16072 [58], which defines a minimum percentage reduction of 50% for a mortar to be considered waterproof.

The higher the percentage of residue, the greater the absorption by capillarity, i.e. the material becomes more permeable and this behavior can be detrimental depending on the application. In addition, as the (w/c) ratio is low, the waste tends to absorb more water, segregating the particles inside the material. This segregation may have been one of the factors behind the increase in capillary absorption [59].

Water absorption by capillarity may also be related to the tortuosity of the pores in the cement matrix. In this case, greater tortuosity makes water permeation more difficult [59, 60].

According to BOTAS [61], capillarity can be analyzed in terms of the initial speed of absorption and in terms of the total amount of water absorbed. Mortars with smaller pore sizes result in lower initial absorption speeds, but a greater amount of water absorbed. On the other hand, the connectivity of the porous network, as well as the open porosity itself, are properties that condition the absorption of water by capillarity, which is one of the main factors responsible for the degradation of mortar coatings.

The results are shown in Table 8 and graphically in Figure 9. The capillary rise of water in the mortars is shown in Figure 10.

**Table 8.** Absorption of water by capillarity, in  $\text{g}/\text{cm}^2$ , as a function of cement replacement content with CV or SP

Time (hours)	Clay						
	REF	CZ 6%	CZ 16%	CZ 26%	SP 6%	SP 16%	SP 26%
0	0	0	0	0	0	0	0
6	0.37	0.32	0.501	0.41	0.43	0.47	0.56
24	0.52	0.43	0.6 97	0.6 2	0.56	0.59	0.71
48	0.6 2	0.51	0.841	0.72	0.6 8	0.76	0.85
72	0.6 3	0.53	0.913	0.76	0.72	0.79	0.93

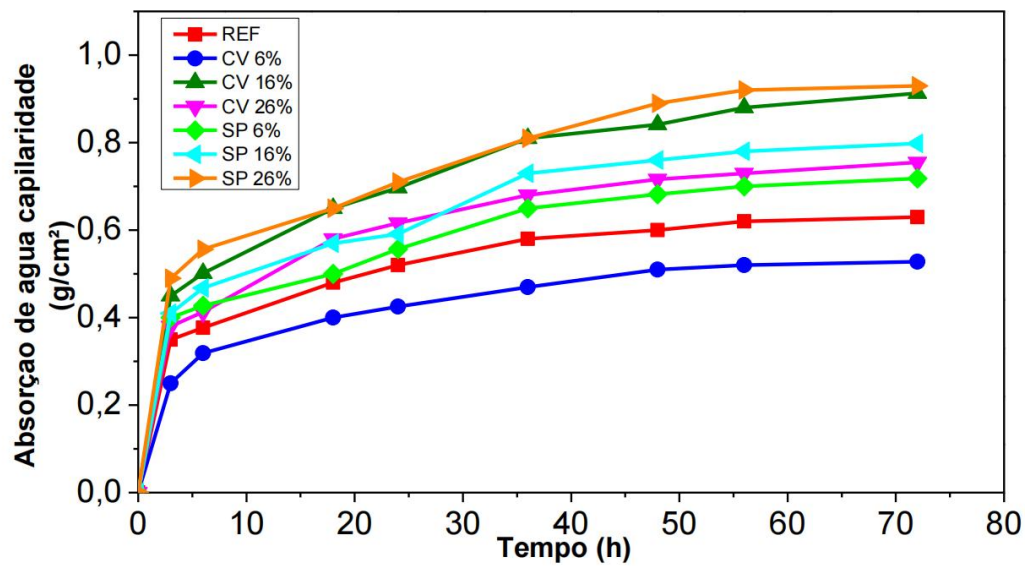


**Figure 9.** Absorption of water by capillarity, in  $\text{g}/\text{cm}^2$ , as a function of cement replacement content with CV or SP.

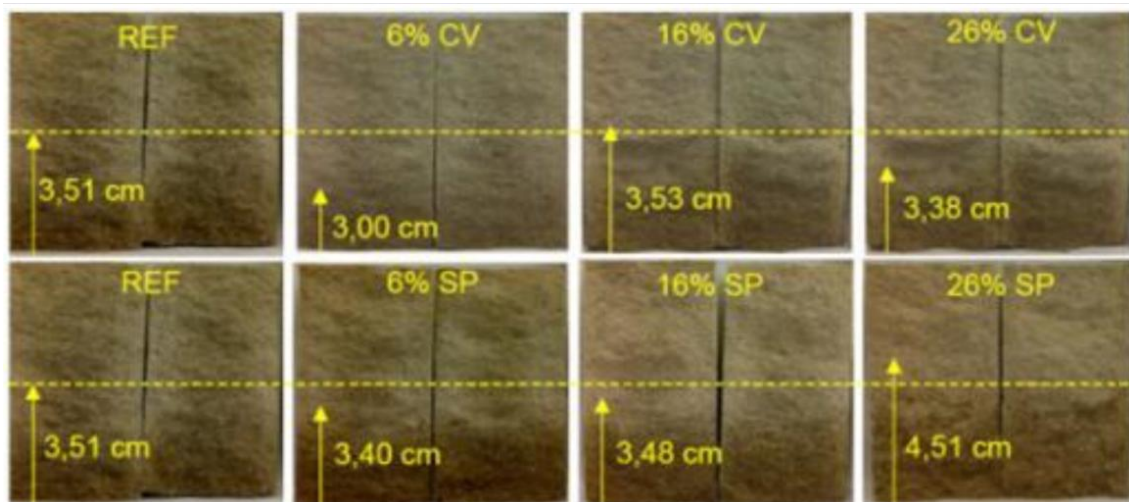


**Figure 10.** Cementitious mortars broken diametrically to measure water rise.

#### 4. Conclusions

In this work, mortars based on Portland cement were formulated with partial substitution by waste from thermoelectric generation. In accordance with the proposed objectives, it was concluded that:

- The characterization study showed that the fly ash waste consists of quartz, mullite and hematite and the FGD by-product consists of calcium sulphate and traces of quartz. The ash can be considered a pozzolanic material.
- Replacing Portland cement with 6% fly ash by mass increases the mortar's axial compressive strength by 5%, resulting in a reduction in cement consumption of 187.2 kg/m<sup>3</sup>. In addition, water absorption was lower in this formulation.
- Fly ash improves the durability of mortars due to the consumption of calcium hydroxide (Ca(OH)<sub>2</sub> or portlandite) and the refinement of pores.
- The curing time interacts with the mortar design and the replacement content.
- No improvements were seen in the mortars with SP additions.
- The use of the fly ash used in this study to replace Portland, limited to 6% by mass, is a viable option for the cement industry, given the economic and environmental advantages it offers. The reduction in clinker consumption and the proper disposal of industrial waste justify the growing use of this waste, as it brings Portland cement and thermoelectric generation into line with the precepts of sustainability and encourages the mitigation of the environmental liabilities of waste-generating companies.

#### Conflicts of Interest

The author declares no conflicts of interest regarding the publication of this paper.

#### References

- [1] TREVISOL, C.A., SILVA, P.R.P., PAULA, M.M.S., et al. "Avaliação de inibidores de corrosão para estruturas de concreto armado", *Revista Matéria UFRJ*, 22, n°. 4, 2017.
- [2] GASPARETTO, A., PANTOJA, J.C., RAMIRES, F.B. "Metodologia para inspeção e avaliação da segurança e durabilidade de estruturas de concreto armado", *Brazilian Journal of Development*, 7.1: 4942-4960, 2021.
- [3] TINOCO, M.P., SILVA, F.A. "Viabilidade da aplicação de compósitos do tipo SHCC para melhoria da durabilidade de estruturas de concreto", *Gestão e Gerenciamento*, 13.13: 52-59, 2020.
- [4] OLIVEIRA, J., SERRA, F.A., et al "Análise da substituição do aço por bambu em estruturas de concreto armado", *Brazilian Journal of Development*, 6.9: 72453-72467. 2020.
- [5] UENDE, S.B., SALOMÃO, P.E.A., LAUAR, G.T., RIBEIRO, P. T."Reutilização do concreto como contribuição para a sustentabilidade na construção civil", *Revista Multidisciplinar do Nordeste Mineiro-Unipac*, ISSN 2178: 6925. 2018.
- [6] BARROS, E., FUCALE, S. "O Uso de Resíduos da Construção Civil como agregados na Produção de Concreto", *Revista de Engenharia e Pesquisa Aplicada*, v. 2, n. 1, 2016.
- [7] CAPELIN, L.J., MORAES, K.K., ZAMPIERI, J.P, et al "Avaliação dos Efeitos da Fibra de Coco e da Microcelulose Cristalina nas Propriedades de Argamassas Cimentícias", *Revista Matéria UFRJ*, v. 25, n. 1, 2020.
- [8] PEREIRA, A.M., SILVA, C.A.R., QUEIROZ, D.C.A.M., et al "Estudo das propriedades mecânicas do concreto com adição de cinza de casca de arroz", *Revista Matéria UFRJ*, v. 20, n. 1, 2015.
- [9] SALES, A., LIMA, S.A. "Use of Brazilian sugarcane bagasse ash in concrete as sand replacement", *Waste Management*, v. 30, n. 6, p. 1114-1122, 2010.
- [10] MATOS, P.R., JUNCKES, R., PRUDÊNCIO, L.R. "Influência do uso de cinza volante na elevação adiabática de temperatura e resistência à compressão de concretos", *Revista Matéria UFRJ*, v. 24, n. 2, 2019.

- [11] COSTA, F.L. "Influência do uso de aditivo acelerador de resistência baseado em nitrato de cálcio no desempenho de argamassas de cimento Portland com adição de cinza volante", *Revista Matéria UFRJ*, v. 23, n. 3, 2018.
- [12] KNISS, C.T., COSTA, P.R., QUONIAM, L., et al "Utilização do resíduo resultante da combustão de carvão mineral em usinas termelétricas na produção de novos materiais: uma análise a partir de artigos científicos e de patentes", *Revista de Gestão social e ambiental*, 13.1: 76-93, 2019.
- [13] SALUM, P.L. "Efeito da elevação de temperatura sobre a resistência à compressão de concretos massa com diferentes teores de cinza volante", Dissertação de M.Sc, Universidade Federal de Santa Catarina, Centro Tecnológico, Programa de Pós-Graduação em Engenharia Civil, Florianópolis. 2016.
- [14] WITZKE, F.B., CORREIA, S.L., MEDEIROS, R.A. "Abrasão superficial de concretos contendo cinza volante em substituição parcial ao cimento Portland", *Revista Técnico-Científica*, 21. 2019.
- [15] FELTRIN, C.S., ISAIA, G.C. e LUBECK, A. "Efeitos sinérgicos entre adições minerais na resistência e microestrutura de concretos", *IBRACON Structures and Materials Journal*, 13.6. 2020.
- [16] DOURADO, K.C.A., MOTA, J.M.F., BARBOSA, F.R., et al "Influência da adição de pozolana em concretos moldados na região de Caruaru" In: 9º Simpósio Internacional de estruturas, geotecnia y materiales de construcción Pernambuco, 2018. Anais [...]. Pernambuco, 2018.
- [17] ALTHEMAN, D., FERREIRA, G., MONTINI, M., et al "Avaliação de Cinza volante de carvão mineral em matrizes cimentícias", *Revista IBRACON de Estruturas e Materiais*, 1320-1337, 2017.
- [18] PACHECO, T.F., SHASAVANDI, A., JALALI, S. "Eco Efficient Concrete Using Industrial Wastes". A Review In: Materials Science Forum p 581-586. Portugal. 2013.
- [19] DUARTE, D., PELISSER, F., PETERSON, M. "Propriedades do concreto com adição de cinza volante e cinza pesada" In: 1º Congresso Internacional de Tecnologias para o Meio Ambiente, Bento Gonçalves, 2008.
- [20] SANTANA, R.A.A. "Avaliação do uso dos subprodutos da dessulfurização semi-seca dos gases da combustão da termelétrica do Pecém como insumo para a construção civil", Dissertação M.Sc, Universidade Federal do Ceará, Fortaleza, 2018.
- [21] ASSOCIAÇÃO BRASILEIRA DE NORMAS TÉCNICAS. NBR 5736: Cimento Portland Pozolânico Rio de Janeiro: ABNT, 1991.
- [22] ASSOCIAÇÃO BRASILEIRA DE NORMAS TÉCNICAS. NBR NM 18: Agregados - Determinação da composição granulométrica Rio de Janeiro: ABNT, 2012.
- [23] ASSOCIAÇÃO BRASILEIRA DE NORMAS TÉCNICAS. NBR NM 11-2: Cimento Portland - Análise química - Método optativo para determinação de óxidos principais por complexometria Parte 2: Rio de Janeiro: ABNT, 2009.
- [24] ASSOCIAÇÃO BRASILEIRA DE NORMAS TÉCNICAS. NBR NM 15: Cimento Portland - Análise química - Determinação de resíduo insolúvel Rio de Janeiro: ABNT, 2012.
- [25] ASSOCIAÇÃO BRASILEIRA DE NORMAS TÉCNICAS. NBR NM 13: Cimento Portland - Análise química - Determinação de óxido de cálcio livre pelo etileno glicol Rio de Janeiro: ABNT, 2012.
- [26] ASSOCIAÇÃO BRASILEIRA DE NORMAS TÉCNICAS. NBR NM 23: Cimento Portland - Análise química - Cimento Portland e outros materiais em pó - Determinação da massa específica Rio de Janeiro: ABNT, 2001.
- [27] ASSOCIAÇÃO BRASILEIRA DE NORMAS TÉCNICAS. NBR NM 76: Cimento Portland - Determinação da finura por meio da peneira 75 µm (nº 200) - Método de ensaio Rio de Janeiro: ABNT, 1998.
- [28] ASSOCIAÇÃO BRASILEIRA DE NORMAS TÉCNICAS. NBR 11579: Cimento Portland - Determinação da finura pelo método de permeabilidade ao ar (Método de Blaine) Rio de Janeiro: ABNT, 1991.

- [29] ASSOCIAÇÃO BRASILEIRA DE NORMAS TÉCNICAS. NBR NM 43: Cimento Portland - Determinação da pasta de consistência normal Rio de Janeiro: ABNT, 2003.
- [30] ASSOCIAÇÃO BRASILEIRA DE NORMAS TÉCNICAS. NBR NM 65: Cimento Portland - Determinação do tempo de pega. Rio de Janeiro: ABNT, 2003.
- [31] ASSOCIAÇÃO BRASILEIRA DE NORMAS TÉCNICAS. NBR 11582: Cimento Portland - Determinação da expansibilidade de Le Chatelier - Método de ensaio. Rio de Janeiro: ABNT, 2012.
- [32] ASSOCIAÇÃO BRASILEIRA DE NORMAS TÉCNICAS. NBR 7215: Cimento Portland - Determinação da resistência à compressão Rio de Janeiro: ABNT, 2019.
- [33] ASSOCIAÇÃO BRASILEIRA DE NORMAS TÉCNICAS. NBR 7211: Agregados para Concreto – Especificações. Rio de Janeiro: ABNT, 2005.
- [34] MALHERBE, C., HUTCHINSON, I.B., McHUGH, H.L., et al "Minerals and microstructure identification using Raman instruments: Evaluation of field and laboratory data in preparation for space mission", *Journal of Raman Spectroscopy*, v. 51, n. 9, p. 1613-1623, 2020.
- [35] Database of Raman spectroscopy, X-ray diffraction and chemistry of minerals. Disponível em: <https://rruff.info/> Acesso em 01 ago.2020.
- [36] ASSOCIAÇÃO BRASILEIRA DE NORMAS TÉCNICAS. NBR 7181: Solo – Análise granulométrica Rio de Janeiro: ABNT, 2018.
- [37] ASSOCIAÇÃO BRASILEIRA DE NORMAS TÉCNICAS. NBR 9779: Argamassa e concreto endurecidos. Determinação da absorção de água por capilaridade, índice de vazios e massa específica: Método de ensaio Rio de Janeiro: ABNT, 2012.
- [38] HOPPE, F.J., GOBBI, A., QUARCIONI, V.A., et al "Atividade pozolânica de adições minerais para cimento Portland (Parte I): Índice de atividade pozolânica (IAP) com cal, difração de raios-X (DRX), termogravimetria (TG/DTG) e Chapelle modificado", *Revista Matéria UFRJ*, v. 22, nº3. 2017.
- [39] YAN, K., GUO, Y., MA, Z.Z., et al "Quantitative analysis of crystalline and amorphous phases in pulverized coal fly ash based on the Rietveld method", *Journal of Non-Crystalline Solids*, v. 483, p. 37-42, 2018.
- [40] KRÓL, M., ROŽEK, P., MOZGAWA, W. "Synthesis of the Sodalite by Geopolymerization Process Using Coal Fly Ash", *Polish Journal of Environmental Studies*, v. 26, n. 6, 2017.
- [41] AZEVEDO, A.G.S. STRECKER, K., BARROS, L.A., et al "Effect of curing temperature, activator solution composition and particle size in brazilian fly-ash based geopolymer production", *Materials Research*, v. 22, 2019.
- [42] PEREIRA, L.F.S. "Estudo da reciclagem de cinza volante para produção de agregado sintético utilizando reator de leito fixo", Dissertação M.Sc, Universidade Federal do Pará – Instituto de Tecnologia – ITEC – Programa de Pós Graduação em Engenharia Química. Belém do Pará – PA. 2016.
- [43] LI, J., et al "Potential utilization of FGD gypsum and fly ash from a Chinese power plant for manufacturing fire-resistant panels", *Construction and Building Materials*, v. 95, p. 910-921, 2015.
- [44] MIAO, M., FENG, XIN., WANG, GANGLING., et al "Direct transformation of FGD gypsum to calcium sulfate hemihydrate whiskers: preparation, simulations, and process analysis", *Particuology*, v. 19, p. 53-59, 2015.
- [45] GUPTA, V., PATHAK, D.K., DIDDIQUE, S., et al "Study on the mineral phase characteristics of various Indian biomass and coal fly ash for its use in masonry construction products", *Construction and Building Materials*, v. 235, p. 117413, 2020.



- [46] SINGH, N., SHEHNAZDEEP., BHARDWAJ, A. "Reviewing the role of coal bottom ash as an alternative of cement", *Construction and Building Materials*, v. 233, p. 117276, 2020.
- [47] SUN, H., TAN, D., PENG, T., et al. "Preparation of calcium sulfate whisker by atmospheric acidification method from flue gas desulfurization gypsum", *Procedia Environmental Sciences*, 31, 621-626, 2016.
- [48] CAILLAHUA, M.C., MOURA, F.J. "Technical feasibility for use of FGD gypsum as an additive setting time retarder for Portland cement", *Journal of Materials Research and Technology*, 7.2: 190-197, 2018.
- [49] MEHTA, P.K, MONTEIRO, P.J.M. "Concreto: microestrutura, propriedades e materiais", São Paulo: IBRACON, 2008.
- [50] COSTA, A.B."Potencial Pozolânico da Cinza Volante como Material de Substituição Parcial de Cimento", Trabalho de Conclusão de Curso apresentado ao Centro de Ciências Exatas e Tecnológicas da UNIVATES, 2008.
- [51] LACERDA, L.V. "Síntese e caracterização de zeólita tipo sodalita obtida a partir de cinzas volantes de carvão mineral utilizado na usina termoeletrica de Candiota-RS", Dissertação de M.Sc, Escola de Engenharia, Universidade Federal do Rio Grande do Sul, Porto Alegre, 2015.
- [52] DIAS, Y.R., RODRIGUES, R., MUNIZ, A.R.C. "Estudo da adsorção em leito fixo de cinzas volantes na remoção de compostos de enxofre do gás obtido na gaseificação do carvão mineral de Candiota-RS", In: V Congresso Brasileiro de Carvão Mineral Criciúma, 2017. Anais [...]. Criciúma, 2017.
- [53] ZERBINO, R., GIACCIO, G., ISAlA, G.C. "Concrete incorporating rice-husk ash without processing", *Construction and Building Materials*, v. 25, n. 1, pp. 371-378, January 2011.
- [54] HOANG, K., JUSTNES, H., GEIKER, M., "Early age strength increase of fly ash blended cement by a ternary hardening accelerating admixture", *Cement and Concrete Research*, v.81, pp. 59-69, 2016.
- [55] TASHIMA, M.M. Cinza de casca de arroz altamente reativa: método de produção, caracterização físico-química e comportamento em matrizes de cimento Portland, dissertação de M.Sc., FEIS/UNESP, Ilha Solteira, SP, Brasil, 2006.
- [56] KHATIB, J.M., WRIGHT, L., MANGAT, P.S. "Mechanical and physical properties of concrete containing FGD waste", *Magazine of concrete Research*, v. 68, n. 11, p. 550-560, 2016.
- [57] MEDEIROS, J. R. A., MUNHOZ, G. S., MEDEIROS, M. H. F. "Correlations between water absorption, electrical resistivity and compressive strength of concrete with different contents of pozzolan", *Revista ALCONPAT*, 9.2: 152-166, 2019.
- [58] ASSOCIAÇÃO BRASILEIRA DE NORMAS TÉCNICAS. NBR 16072: Argamassa impermeável Rio de Janeiro: ABNT. 2012.
- [59] OLSSON, N., BAROGHEL, B.V., NILSSON, L.O., et al "Non-saturated ion diffusion in concrete – A new approach to evaluate conductivity measurements", *Cement and Concrete Composites*, 40:40-47, 2013.
- [60] MEDEIROS, J.R.A., LIMA, M.G. "Electrical resistivity of unsaturated concrete using different types of cement", *Construction and Building Materials*, 107:11-16, 2016.
- [61] BOTAS, S.M.S. "Avaliação do comportamento de argamassas em climas frios", Dissertação de MSc., Universidade Nova de Lisboa, Faculdade de Ciências e Tecnologia-Lisboa, 2019.